Stroma AReactive Invasion Front Areas (SARIFA) - a new prognostic biomarker in gastric cancer related to tumor promoting adipocytes

Bianca Grosser, Marie Isabelle Glückstein, Christine Dhillon, Stefan Schiele, Sebastian Dintner, Alison VanSchoiack, David Kroeppler, Benedikt Martin, Andreas Probst, Dmytro Vlasenko, Gerhard Schenkirsch, Bruno Märkl

Angaben zur Veröffentlichung / Publication details:

Grosser, Bianca, Marie Isabelle Glückstein, Christine Dhillon, Stefan Schiele, Sebastian Dintner, Alison VanSchoiack, David Kroeppler, et al. 2021. "Stroma AReactive Invasion Front Areas (SARIFA) - a new prognostic biomarker in gastric cancer related to tumor promoting adipocytes." *The Journal of Pathology* 256 (1): 71–82. https://doi.org/10.1002/path.5810.

Journal of Pathology
J Pathol January 2022; **256:** 71–82
Published online 22 October 2021 in Wiley Online Library (wileyonlinelibrary.com) DOI: 10.1002/path.5810

ORIGINAL PAPER

Stroma AReactive Invasion Front Areas (SARIFA) – a new prognostic biomarker in gastric cancer related to tumor-promoting adipocytes

Bianca Grosser[1], Marie-Isabelle Glückstein[1], Christine Dhillon[1], Stefan Schiele[2], Sebastian Dintner[1], Alison VanSchoiack[3], David Kroeppler[3], Benedikt Martin[1], Andreas Probst[4], Dmytro Vlasenko[5], Gerhard Schenkirsch[6] and Bruno Märkl[1]*

[1] *General Pathology and Molecular Diagnostics, Medical Faculty, University of Augsburg, Augsburg, Germany*
[2] *Institute of Mathematics and Computational Statistics, University of Augsburg, Augsburg, Germany*
[3] *NanoString Technologies, Inc, Seattle, WA, USA*
[4] *Department of Gastroenterology, University Hospital Augsburg, Augsburg, Germany*
[5] *General, Visceral and Transplantation Surgery, University Hospital of Augsburg, Augsburg, Germany*
[6] *Tumor Data Management, University Hospital Augsburg, Augsburg, Germany*

**Correspondence to: B Märkl, Institut für Pathologie und Molekulare Diagnostik, Universitätsklinikum Augsburg, Stenglinstraße 2, 86156 Augsburg, Germany. E-mail: bruno.maerkl@uka-science.de*

Abstract

Compared to other malignancies, there is a lack of easy-to-evaluate biomarkers for gastric cancer, which is associated with an adverse clinical outcome in many cases. Here, we present Stroma AReactive Invasion Front Areas (SARIFA) as a new histological prognostic marker. We defined SARIFA as the direct contact between a cluster of tumor glands/cells comprising at least five tumor cells and inconspicuous surrounding adipose tissue at the invasion front. A total of 480 adenocarcinomas of the stomach and the gastroesophageal junction from two different collections were classified according to SARIFA. To understand the potential underlying mechanisms, a transcriptome analysis was conducted using digital spatial profiling (DSP). It was found that 20% of the tumors were SARIFA-positive. Kappa values between the three pathologists were good in both collections: 0.74 and 0.78. Patients who presented SARIFA-positive tumors had a significantly lower overall survival in Collections A (median: 20.0 versus 44.0 months; $p = 0.014$, $n = 160$) and B (median: 15.0 versus 41.0 months; $p < 0.0001$, $n = 320$). SARIFA positivity emerged as a negative independent prognostic factor for overall survival (HR 1.638, 95% CI 1.153–2.326, $p = 0.006$). Using DSP, the most upregulated genes in SARIFA-positive cases were those associated with triglyceride catabolism and endogenous sterols. *COL15A1*, *FABP2*, and *FABP4* were differentially expressed in positive cases. At the protein level, the expression of proteins related to lipid metabolism was confirmed. SARIFA combines low inter-observer variability, minimal effort, and high prognostic relevance, and is therefore an extremely promising biomarker related to tumor-promoting adipocytes in gastric cancer.

Keywords: gastric cancer; Stroma Areactive Invasion Front Areas; SARIFA; biomarker; histopathology; digital spatial profiling

Received 24 July 2021; Revised 14 September 2021; Accepted 24 September 2021

Conflict of interest statement: AV is an employee and also a shareholder of NanoString Technologies, Inc. No other conflicts of interest were disclosed.

Introduction

Gastric cancer is ranked as the sixth most common cancer entity worldwide, having accounted for approximately 780 000 cancer-associated deaths in 2018 [1]. So far, the best parameter for predicting prognosis, and therefore therapy, in gastric cancer patients is TNM staging. The factors that are relevant for determining the prognosis of gastric carcinomas are local infiltration depth, locoregional lymph node involvement, distant metastases, and vascular invasion [2–4]. Additionally, diffuse Laurén subtype and proximal tumor localization are also known negative prognostic factors for gastric cancer [5–7]. The introduction of perioperative chemotherapy after 2005 has improved the outcome in stage 2 and 3 gastric cancers, with a median survival of 50 months versus 34 months [8]. However, the prognosis of gastric cancer is still poor and has a 5-year survival rate that has not changed during the period between 2000 and 2014, with survival rates being between 31.4% and 33.5% in Germany [9]. To improve the prognosis estimation in gastric cancer beyond TNM staging, histomorphology-based concepts, such as tumor budding and the tumor–stroma ratio (TSR), have already been investigated. Unlike the case of colorectal cancer, such biomarkers have not reached general acceptance or been recommended in routine diagnostics [10–12]. Moreover, the molecular classification of the Cancer Genome Atlas (TCGA) identified distinct subgroups of

gastric carcinomas that were associated with specific clinicopathological characteristics, but they failed to robustly predict patient survival [13]. So far, only microsatellite instability (MSI) and programmed death-ligand 1 (PD-L1) status have gained acceptance as prognostic biomarkers in gastric cancer [14]. Therefore, there is still a need to identify biomarkers for improving the prognostic prediction and therapy stratification in gastric cancer.

During our investigations addressing the prognostic value of the TSR in colon cancer, we recognized that in a certain portion of cases the tumor formations come into direct contact with adipose cells that lack a stromal reaction. Quite recently, we were able to confirm our hypothesis that this morphological feature, which we referred to as Stroma AReactive Invasion Front Areas (SARIFA), can serve as an adverse prognostic factor for the outcome in colon cancer [15]. The advantage of this biomarker is its simplicity; it does not need any additional testing or expenditure, offers ease of learning, has minimal time requirements, and provides extraordinarily low interobserver variability. The identification of this phenomenon in colon cancer gave rise to the question of whether this occurs in other cancer entities as well. The fact that SARIFA represents the areas in which there is direct contact between the tumor cells and the local mesenchymal tissue without intervening reactive collagen raises the question of whether this enables an interaction that has tumor-promoting effects. Considering the observation that obesity is associated with an increased incidence and aggressivity of malignant tumors, there is increasing interest in the crosstalk between the tumor cells and adipocytes. Indeed, the experimental data indicate that tumors gain advantages from a direct interaction with adipocytes [16].

The aim of the present study was to investigate the prognostic significance of SARIFA in a limited test collection of adenocarcinomas of the stomach and the gastroesophageal junction ($n = 160$) and to further validate the results in a larger collection of 320 patients. In addition, the possible underlying mechanisms or differences between negative and positive cases were investigated using transcriptome and subsequent immunohistochemical analyses.

Materials and methods

Patients

Patient collection A served as the test collection and consisted of surgical resection specimens from 160 patients with adenocarcinomas of the stomach and the gastroesophageal junction (AEG II and III according to Siewert and Stein [17]) that at least presented infiltration of the submucosa (pT1b). These patients were treated between 2005 and 2018 at the Department of Surgery of the University Hospital Augsburg. In total, 69% of the tumors had been treated with surgery alone and 31% of the patients received neoadjuvant chemotherapy (CTx). Collection B was formed as the validation collection and comprised 320 patients selected using the same inclusion criteria as those used for Collection A. Among these, 28% of the patients received neoadjuvant CTx, and their detailed clinicopathological characteristics have been summarized in Tables 1 and 2.

The response to preoperative CTx was determined histopathologically and classified into three tumor-regression grades (TRGs) – TRG1b, TRG2, and TRG3 – which corresponded to <10%, 10–50%, and >50% residual tumor cells [18]. All patients were treated with chemotherapeutic regimes based on platinum/5-fluorouracil (5-FU) (Table 1). Further, all surgical approaches included an abdominal D2 lymphadenectomy [19].

The follow-up data were obtained from the tumor data management of the University Hospital of Augsburg, and the median follow-up was calculated using the inverse Kaplan–Meier method [20]. The primary endpoint of the study was overall survival (OS), which was defined as the time elapsed between the date of diagnosis and the death of the patient due to any cause. Patients with an OS of less than 30 days were excluded from the study.

The study was approved by the ethical committee of the Ludwig Maximilian University of Munich (reference: 20-0922) and was performed in accordance with the Declaration of Helsinki. According to the ethics vote of the institutional review boards of the Ludwig Maximilian University of Munich (reference: 20-0922), a declaration of consent was not necessary.

Definition and assessment of SARIFA

SARIFA was evaluated based on entire slide sections that covered about 220 mm^2. We have defined SARIFA as an area located at the invasion front (IF) in which a tumor gland or a group of at least five tumor cells directly approach adipocytes without separating stroma. In addition, SARIFA was said to be present when tumor cells were directly adjacent to local tissue, such as the smooth muscle in muscularis propria, without a stromal reaction, such as fibroblastic proliferation, collagen formation, or a histiocytic reaction. We classified tumors that presented these characteristics as SARIFA-positive and the others as SARIFA-negative. Even if only a single SARIFA was present (e.g. a single tumor gland surrounded directly by inconspicuous adipose tissue), we classified the tumor as SARIFA-positive. The first (FA), third (TA), and last author (LA) independently assessed all tumors. They did not have access to each other's results or the clinical data. An exemplary tumor slide preselected by FA was used for assessment in each case. Further, any discrepant results were discussed using a multi-head microscope, and a consensus was reached. Example images are presented in Figure 1.

Tissue microarray construction and TCGA classification

For the classification according to the TCGA, tissue microarrays (TMAs) were constructed. Tumors were

Table 1. Clinicopathological characteristics – Collection A.

Variable		$n = 160$		SARIFA-positive ($n = 24$)		SARIFA-negative ($n = 136$)		*P* value
Median age (range), years		70.5 (30–95)		71 (40–87)		70.5 (30–95)		0.100
Median follow-up (95% CI), months		56.0 (44.8–67.2)		80.0 (NA)		54.0 (41.2–66.8)		0.462
Sex								0.549
	Female	58	36%	10	42%	48	35%	
	Male	102	64%	14	58%	88	65%	
T status								**<0.001**
	pT1/2	61	38%	1	4%	60	44%	
	pT3/4	99	62%	23	96%	76	56%	
N status								0.088
	Negative	58	36%	5	21%	53	39%	
	Positive	102	64%	19	79%	83	61%	
Distant metastasis								**0.009**
	No	83	52%	7	29%	76	56%	
	Yes	67	42%	16	67%	51	38%	
	NA	10	6%	1	4%	9	7%	
Grading								0.682
	Low grade	54	34%	7	29%	47	35%	
	High grade	104	65%	16	67%	88	65%	
	NA	2	1%	1	4%	1	1%	
Vascular invasion								0.184
	Negative	145	91%	20	83%	125	92%	
	Positive	15	9%	4	17%	11	8%	
Lymphovascular invasion								**0.047**
	Negative	108	68%	12	50%	96	71%	
	Positive	52	33%	12	50%	40	29%	
Laurén classification								0.265
	Intestinal	90	56%	11	46%	79	58%	
	Non-intestinal	70	44%	13	54%	57	42%	
Localization								1.000
	Proximal	40	25%	6	25%	34	25%	
	Non-proximal	120	75%	18	75%	102	75%	
R status								0.389
	R0	141	88%	20	83%	121	89%	
	R1	13	8%	3	13%	10	7%	
	Rx	6	4%	1	4%	5	4%	
TCGA								0.218
	EBV^+	12	8%	0	0%	12	9%	
	MMRD	18	11%	2	8%	16	12%	
	GS	35	22%	4	17%	31	23%	
	CIN	46	29%	10	42%	36	26%	
	Non-classifiable	40	25%	7	29%	33	24%	
	NA	9	6%	1	4%	8	6%	
Death								**0.006**
	No	81	51%	6	25%	75	55%	
	Yes	79	49%	18	75%	61	45%	
nCTx								0.811
	No	110	69%	17	71%	93	68%	
	Yes	50	31%	7	29%	43	32%	
TRG								0.150
	1b	5	10%	0	0%	5	12%	
	2	19	38%	1	14%	18	42%	
	3	26	52%	6	86%	20	47%	
CTx regime								0.206
	Cis/Ox/5-FU or Cap	13	26%	0	0%	13	30%	
	Ox +5-FU + Doc	19	38%	2	29%	17	40%	
	Cis + 5-FU + Epi	13	26%	4	57%	9	21%	
	Ox + Epi + Cap	4	8%	1	14%	3	7%	
	Others	1	2%	0	0%	1	2%	

P values are shown for difference between SARIFA-positive and SARIFA-negative tumors; values in bold are statistically significant.
5-FU, 5-fluorouracil; Cap, capecitabine; CIN, chromosomally instable; Cis, cisplatin; Doc, docetaxel; EBV^+, EBV positive; Epi, epirubicin; GS, genomically stable; MMRD, mismatch repair deficient; nCTx, neoadjuvant CTx; Others, combination of Cis/Ox with other agents or crossover between different treatment regimens; Ox, oxaliplatin; Pac, paclitaxel; TCGA, The Cancer Genome Atlas; TRG, tumor regression grade.

classified in analogy to the TCGA classification [13] based on the immunohistochemical expression of PMS2, MSH6, E-cadherin, p53, and EBER-CISH [21,22]. The TMA construction and classification according to the TCGA are described in more detail in the Supplementary materials and methods.

Table 2. Clinicopathological characteristics – Collection B.

Variable		n = 320		SARIFA-positive (n = 72)		SARIFA-negative (n = 248)		P value
Median age (range), years		69.0 (36–91)		70.0 (38–91)		69.0 (36–90)		0.100
Median follow-up (95% CI), months		62.0 (49.6–74.4)		58.0 (26.5–89.5)		63.0 (49.0–77.0)		0.912
Sex								0.533
	Female	103	32%	21	29%	82	33%	
	Male	217	68%	51	71%	166	67%	
T status								**<0.001**
	pT1/2	92	29%	7	10%	85	34%	
	pT3/4	228	71%	65	90%	163	66%	
N status								**0.004**
	Negative	117	37%	16	22%	101	41%	
	Positive	203	63%	56	78%	147	59%	
Distant metastasis								**<0.001**
	No	161	50%	23	32%	138	56%	
	Yes	136	43%	45	63%	91	37%	
	NA	23	7%	4	6%	19	8%	
Grading								0.083
	Low grade	105	33%	17	24%	88	35%	
	High grade	210	66%	52	72%	158	64%	
	NA	5	2%	3	4%	19	8%	
Vascular invasion								**0.017**
	Negative	258	81%	51	71%	207	83%	
	Positive	62	19%	21	29%	41	17%	
Lymphovascular invasion								**0.018**
	Negative	181	57%	32	44%	149	60%	
	Positive	139	43%	40	56%	99	40%	
Laurén classification								0.648
	Intestinal	172	54%	37	51%	135	54%	
	Non-intestinal	148	46%	35	49%	113	46%	
Localization								0.087
	Proximal	90	28%	26	36%	64	26%	
	Non-proximal	230	72%	46	64%	184	74%	
R status								0.095
	R0	265	83%	52	72%	213	86%	
	R1	42	13%	13	18%	29	12%	
	Rx	13	4%	7	10%	6	2%	
TCGA								0.225
	EBV^+	12	4%	4	6%	8	3%	
	MMRD	41	13%	7	10%	34	14%	
	GS	73	23%	12	17%	61	25%	
	CIN	95	30%	26	36%	69	28%	
	Non-classifiable	82	26%	20	28%	62	25%	
	NA	17	5%	3	4%	14	6%	
Death								**0.004**
	No	146	46%	22	31%	124	50%	
	Yes	174	54%	50	69%	124	50%	
nCTx								0.503
	No	230	72%	54	75%	176	71%	
	Yes	90	28%	18	25%	72	29%	
TRG								0.143
	1b	9	10%	0	0%	9	13%	
	2	22	24%	3	17%	19	26%	
	3	59	66%	15	83%	44	61%	
CTx regime								0.505
	Cis/Ox/5-FU or Cap	15	17%	2	11%	13	18%	
	Ox +5-FU + Doc	31	34%	6	33%	25	35%	
	Cis + 5-FU + Epi	31	34%	9	50%	22	31%	
	Ox + Epi + Cap	11	12%	1	6%	10	14%	
	Others	2	2%	0	0%	2	3%	

P values are shown for difference between SARIFA-positive and SARIFA-negative tumors; values in bold are statistically significant.
5-FU, 5-fluorouracil; Cap, capecitabine; CIN, chromosomally instable; Cis, cisplatin; Doc, docetaxel; EBV^+, EBV positive; Epi, epirubicin; GS, genomically stable; MMRD, mismatch repair deficient; nCTx, neoadjuvant CTx; Others, combination of Cis/Ox with other agents or crossover between different treatment regimens; Ox, oxaliplatin; Pac, paclitaxel; TCGA, The Cancer Genome Atlas; TRG, tumor regression grade.

NanoString GeoMx digital spatial profiling (DSP)

The DSP analysis is described in more detail in the Supplementary materials and methods. Using DSP, we performed a multiplexed and spatially resolved profiling analysis on exemplary SARIFA-positive and SARIFA-negative cases of TMAs (six SARIFA-positive and six

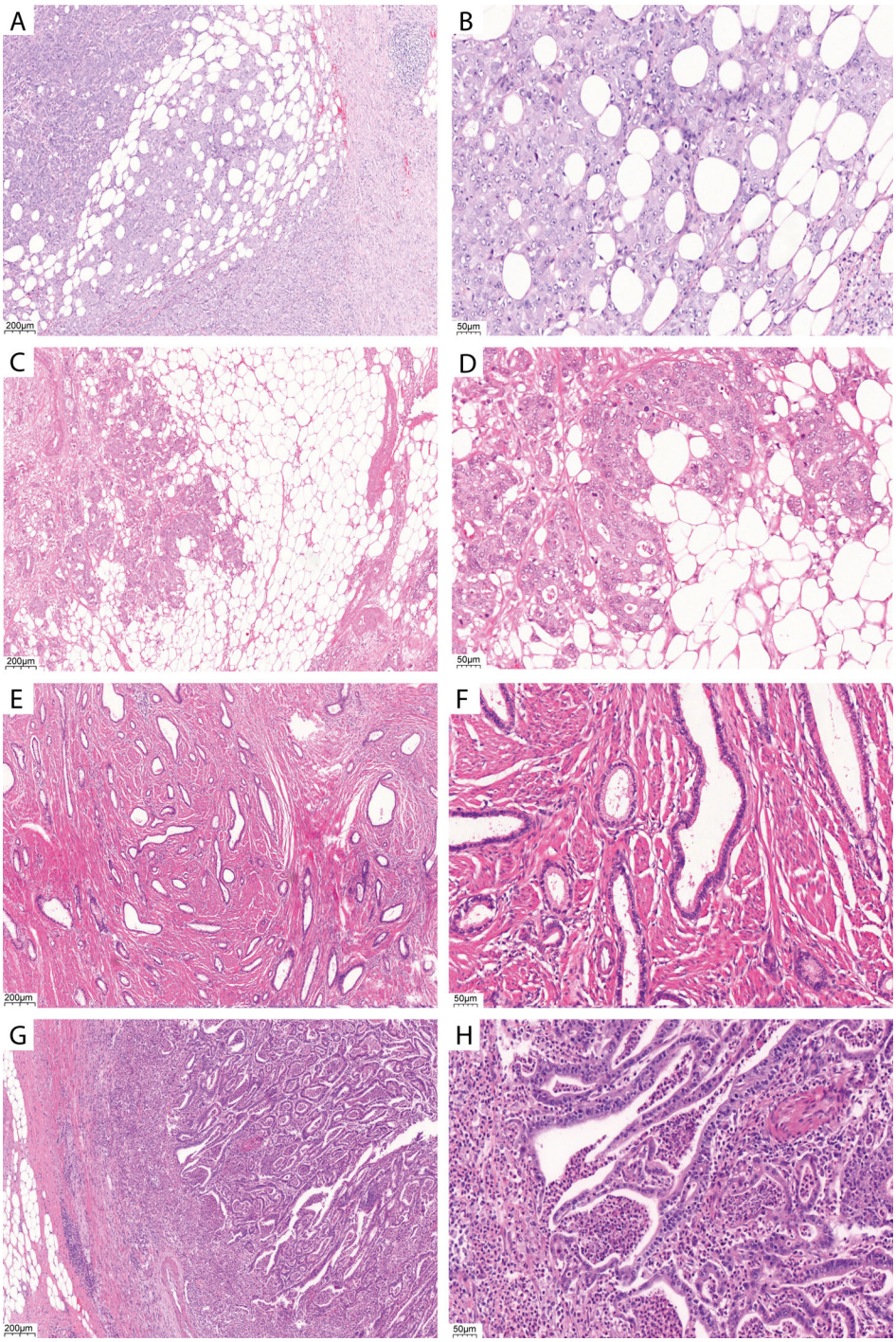

Figure 1. H&E images of SARIFA-positive and SARIFA-negative cases: SARIFA-positive cases (A, C, E: scale bar = 200 µm; B, D, F: scale bar = 50 µm) with tumor cells directly adjacent to local tissue, such as adipocytes (A–D) or smooth muscle in muscularis propria (E, F), without a stromal reaction. SARIFA-negative case at the invasion front (G: scale bar = 200 µm; H: scale bar = 50 µm).

SARIFA-negative cases). DSP technology uses RNA detection probes with ultraviolet (UV) photocleavable indexing oligos for transcriptomic profiling within the selected regions of interest (ROIs). As shown in Figure 3A,B, based on fluorescence imaging to visualize the tumor cells and the corresponding H&E images, ROIs within the SARIFA-positive and SARIFA-negative areas were chosen for multiplex profiling. Sequencing libraries were generated as described previously [23] according to NanoString's GeoMx-NGS Readout Library Prep instructions (NanoString Technologies, Inc, Seattle, WA, USA) and sequenced on an Illumina NovaSeq (Illumina Inc, San Diego, CA, USA).

Immunohistochemical protein expression of differentially expressed genes in DSP analysis and of proteins associated with fatty acid metabolism, hypoxia, and stem cell features

The immunohistochemical expression of FABP4, CD36, CD44, carbonic anhydrase IX, CD68, and Ki67

obtained from 30 SARIFA-positive and 30 SARIFA-negative cases was analyzed on 2 µm whole-slide sections using the primary antibodies listed in supplementary material, Table S1. Staining was performed on the BOND Rx platform using the BOND Polymer Refine Detection kit (Leica Biosystems, Nussloch, Germany). Adequate controls were used for quality control during staining (see supplementary material, Table S1). The staining was assessed separately for the IF and tumor center (TC). For CD36, CD44, and carbonic anhydrase IX, the staining was evaluated using the seven-tier semi-quantitative scoring system (immunoreactive score, IRS) proposed by Remmele and Stegner [24] while taking into account staining intensity and the percentage of positive tumor cells. For FABP4 and Ki67, the percentage of tumor cells positive was assessed. Finally, the abundance of macrophages was assessed through CD68 staining.

Statistical analyses

Chi-squared tests were used for hypothesis testing of differences between relative frequencies. Continuous variables were compared using the Wilcoxon rank-sum test, while correlations were calculated using the Spearman test. Kaplan–Meier estimates of survival rates were compared using log-rank tests, and relative risks were estimated by hazard ratios (HRs) obtained from Cox proportional hazard models. Because overall patient survival was chosen as the study endpoint, an additional comparison of survival curves was performed using the Gehan–Breslow–Wilcoxon (GBW) test, as this gives more weight to early events that are more likely to be cancer-specific. Kappa statistics were used as a measure of inter-observer agreement [25]. Statistical analyses were performed using SPSS version 24 (IBM Corp., Armonk, NY, USA) and R version 4.0.3. Exploratory significance levels (two-tailed) of 5% were used for hypothesis testing. The DSP analysis was conducted using GeoMx Analysis Suite Version 2.2.0.111 (NanoString Technologies, Inc).

Results

For Collection A, the mean age of the patients was 70.5 (range 30.0–95.0) years and the median follow-up time was 56.0 (range 44.8–67.2) months. In total, 49% of the patients died during the follow-up period. Detailed clinicopathological characteristics are summarized in Table 1. Overall, 24 (15%) cases were classified as SARIFA-positive, and 136 (85%) were deemed SARIFA-negative.

For Collection B, the mean age of the 320 patients at the time of diagnosis was 69.0 (range 36.0–91.0) years and the mean follow-up time was 62.0 (range 49.6–74.4) months. Of the 320 patients, 54% died during the follow-up period. Detailed clinicopathological characteristics are provided in Table 2. Overall, 72 (22.5%) tumors were classified as SARIFA-positive, while 248 (77.5%) were classified as SARIFA-negative.

SARIFA presents high inter-observer concordance

The first (FA), third (TA), and last author (LA) independently assessed all the tumors included in this study.

For Collection A, the overall kappa value obtained by all three observers was 0.738 (FA and TA: 0.727; FA and LA: 0.860; TA and LA: 0.636). For Collection B, the overall kappa value obtained by all three observers was 0.775 (FA and TA: 0.839; FA and LA: 0.763; TA and LA: 0.721).

SARIFA and clinicopathological characteristics

The SARIFA-positive tumors were associated with several clinicopathological factors in both collections. An overview of this is presented in Tables 1 and 2 for Collection A and B, respectively. In both collections, SARIFA-positive tumors were associated with an advanced T-stage ($p < 0.01$ for each), distant metastases ($p < 0.01$ for each), and lymphovascular invasion ($p < 0.05$ for each). Additionally, in Collection B, the SARIFA-positive tumors were more frequently found to present positive lymph nodes ($p < 0.01$) and vascular invasion ($p = 0.018$). Further, no association with the molecular TCGA subtypes could be seen in Collection A or B ($p = 0.218$ and 0.225, respectively). As the interaction between adipose tissues and tumor cells has primarily been studied in the context of obesity research, we determined the relationship between SARIFA and patients' body mass index (BMI) in a subgroup of 60 cases (30 SARIFA-positive and -negative cases each). Here, SARIFA was associated with a lower BMI (median: 25 kg/m^2) compared with non-SARIFA patients (median: 27 kg/m^2) ($p = 0.038$).

SARIFA and survival

For Collection A, patients who presented with SARIFA-positive tumors had a significantly lower OS ($p_{\log\ \text{rank}} = 0.014$, Figure 2A; $p_{\text{GBW}} = 0.165$). SARIFA-positive patients had a median survival of 20.0 (11.0–29.0) months as opposed to 44.0 (17.7–70.3) months for SARIFA-negative cases. During the study period, 75% of the patients who had SARIFA-positive tumors died, whereas this was the case for 45% of the SARIFA-negative patients.

For Collection B, patients with SARIFA-positive tumors had a significantly lower OS ($p_{\log\ \text{rank}\ +\text{GBW}} < 0.001$, Figure 2B). The SARIFA-positive cases showed a median survival of 15.0 (6.5–23.5) months, whereas patients with SARIFA-negative tumors had a median survival of 41.0 (21.8–60.2) months. During the study period, 69% of the patients who presented with SARIFA-positive tumors died, whereas this was the case for 50% of the SARIFA-negative patients.

Additionally, SARIFA positivity emerged as an independent negative prognostic factor (HR 1.638, 95% CI

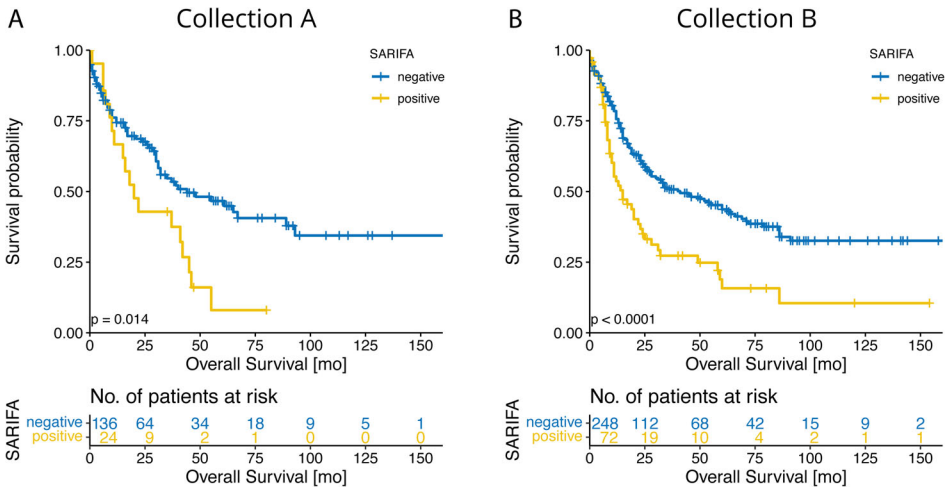

Figure 2. Discrimination of patient survival based on SARIFA status. The Kaplan–Meier curves of patients with SARIFA-positive and SARIFA-negative tumors are shown. (A) Collection A ($n = 160$); (B) Collection B ($n = 320$). *P* value of log-rank test.

1.153–2.326, $p = 0.006$) for OS in Cox regression analyses, which were adjusted according to the known prognostic parameters (age, pT, pN, grading, and lymphovascular and vascular invasion). The results of these analyses are summarized in supplementary material, Table S2.

Subgroup analysis

The subgroup analysis indicated the existence of a negative prognostic effect of SARIFA in primarily resected (HR 1.866, 95% CI 1.350–2.581, $p < 0.001$) and CTx patients (HR 2.003, 95% CI 1.145–3.506, $p = 0.015$). As shown in supplementary material, Table S3, SARIFA is a prognostic factor for intestinal or non-intestinal Laurén subtypes. The negative prognostic effect of SARIFA can especially be seen in non-proximal tumor localization. Regarding the pT stage, only advanced-stage (pT3/4) SARIFA-positive patients showed a worse OS (HR 1.618, 95% CI 1.200–2.180, $p = 0.002$), whereas no differences in terms of survival could be observed during the early stages (pT1/2) (HR 1.201, 95% CI 0.431–3.344, $p = 0.726$). Regarding the subgroups of TCGA, SARIFA was found to be a negative prognostic variable, especially in CIN (HR 1.756, 95% CI 1.106–2.788, $p = 0.017$) and non-classifiable tumors (HR 2.460, 95% CI 1.436–4.216, $p = 0.001$. Detailed information about this may be found in supplementary material, Table S3.

Differentially expressed genes identified using DSP

Using DSP technology, we identified genes that were significantly upregulated at the IF in SARIFA-positive cases compared with SARIFA-negative cases, as shown in Figure 3C. The most interesting upregulated genes in SARIFA-positive cases at the IF included *COL15A1* ($p = 2.3569E-05$), *FABP2* ($p = 0.000226326$), *FABP4* ($p = 0.000763128$), and *FGB* ($p = 0.001792231$). Figure 3 shows the differential expression of *COL15A1* (Figure 3D) and *FABP4* (Figure 3E) with the lowest expression in the SARIFA-negative areas at the IF. *FAPB4* expression increases toward SARIFA-positive centers and again toward SARIFA-positive IFs. The expression of *COL15A1*, *FABP2*, *FABP4*, and *FGB* in the SARIFA-positive and SARIFA-negative areas is demonstrated in Figure 3F.

In pathway analyses, the most upregulated genes in the SARIFA-positive cases were found to be those associated with triglyceride catabolism, endogenous sterols, collagen chain trimerization, and fibrin clot formation.

Immunohistochemical detection of the protein products of differentially expressed genes in DSP analysis, and of proteins associated with hypoxia and stem cell features

We wanted to confirm the differential expression of FABP4, which was identified using DSP analysis, at the protein level. FABP4 was almost exclusively expressed in the SARIFA areas, whereas it was totally absent in the TC, or in non-SARIFA cases at the IF or TC (IF SARIFA versus non-SARIFA $p < 0.001$; Figure 4A). Cancer cells acquire exogenous fatty acids through cell-surface acid translocase, which is also called CD36 [26,27]. CD36 was significantly upregulated at the IF ($p < 0.001$) in SARIFA cases and was almost absent or present at extremely low expression at the TC and in non-SARIFA cases (Figure 4B). To assess the number of tumor-associated macrophages (TAMs), we immunostained for CD68. We observed that the number of $CD68^+$ cells increased at the IF ($p = 0.019$) and in the TC ($p = 0.060$) in SARIFA cases compared with SARIFA-negative tumors (Figure 4F).

To verify whether hypoxia plays a role with regard to SARIFA, we assessed the expression of carbonic anhydrase IX. As shown in Figure 4G, no difference between SARIFA and non-SARIFA cases was observed. In Figure 4H, the expression of CD44 (a marker of stem cell features) is shown. Expression of CD44 was significantly lower at the IF in SARIFA cases ($p < 0.001$) and

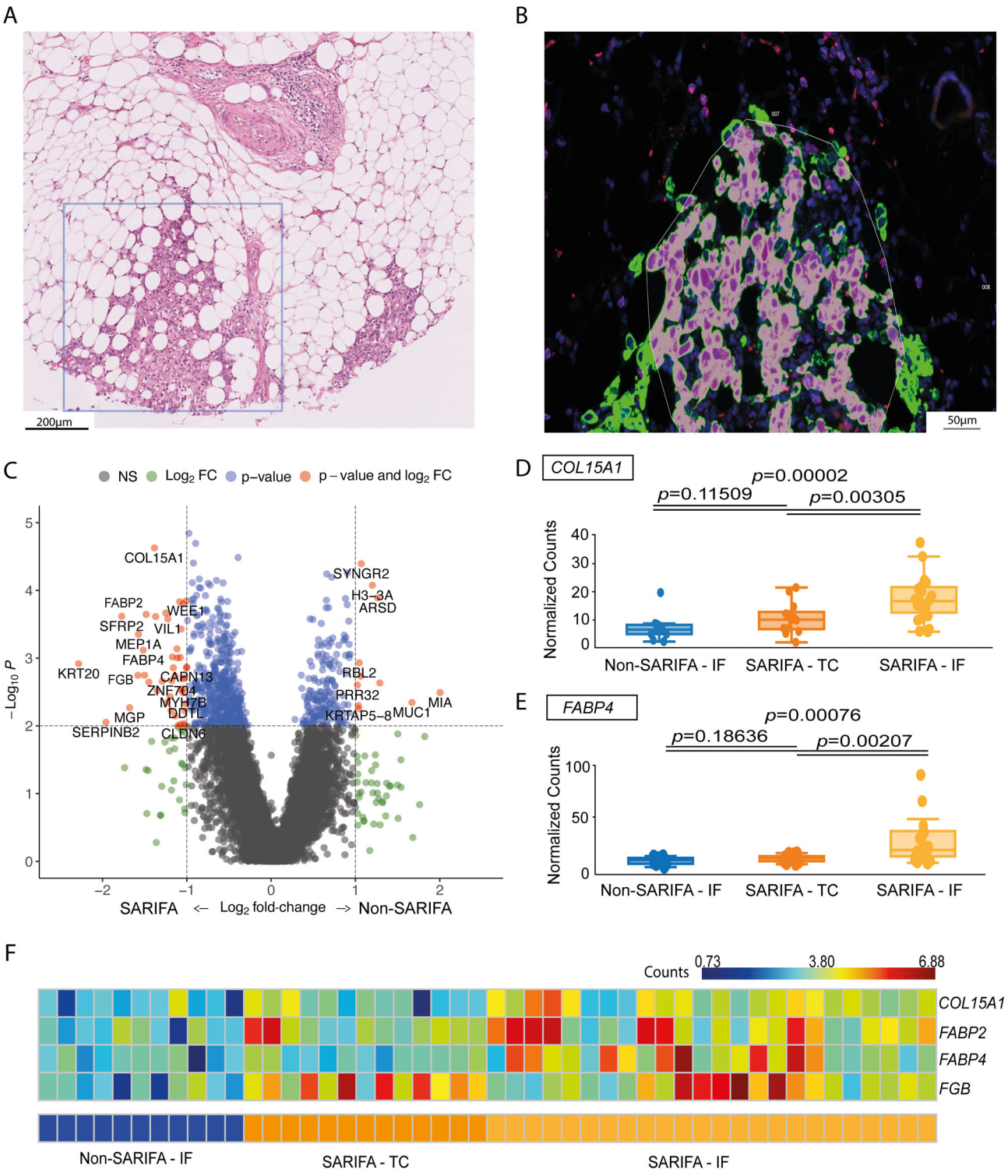

Figure 3. Transcriptome analysis using DSP. (A, B) H&E slide of a TMA core of a SARIFA-positive tumor (A) and serial fluorescence image visualizing the tumor cells in the SARIFA-area. Based on fluorescence imaging, ROIs were chosen for multiplex profiling (B). (C) Volcano plot showing differentially expressed genes between SARIFA-positive and SARIFA-negative cases at the IF in DSP analysis. (D, E) *COL151A* (D) and *FABP4* (E) are significantly differentially expressed in SARIFA-negative, and SARIFA-positive TC and SARIFA-positive IF, showing the highest expression in tumor cells at the IF in SARIFA cases. (F) Heatmap demonstrating the expression (digital counts) of *COL15A1*, *FABP2*, *FABP4*, and *FGB* in all analyzed cases of non-SARIFA cases at the IF, and SARIFA cases in the TC and at the IF.

TC ($p = 0.001$). Based on the proliferation-associated marker Ki67, no difference was seen between the SARIFA and non-SARIFA cases with regard to proliferation activity (Figure 4I).

The expression of FABP4 at the IF showed a significant inverse correlation with CD44 at the IF ($\rho = -0.446$, $p < 0.001$) and in the TC ($\rho = -0.476$, $p < 0.001$). FABP4 IF was found to be positively

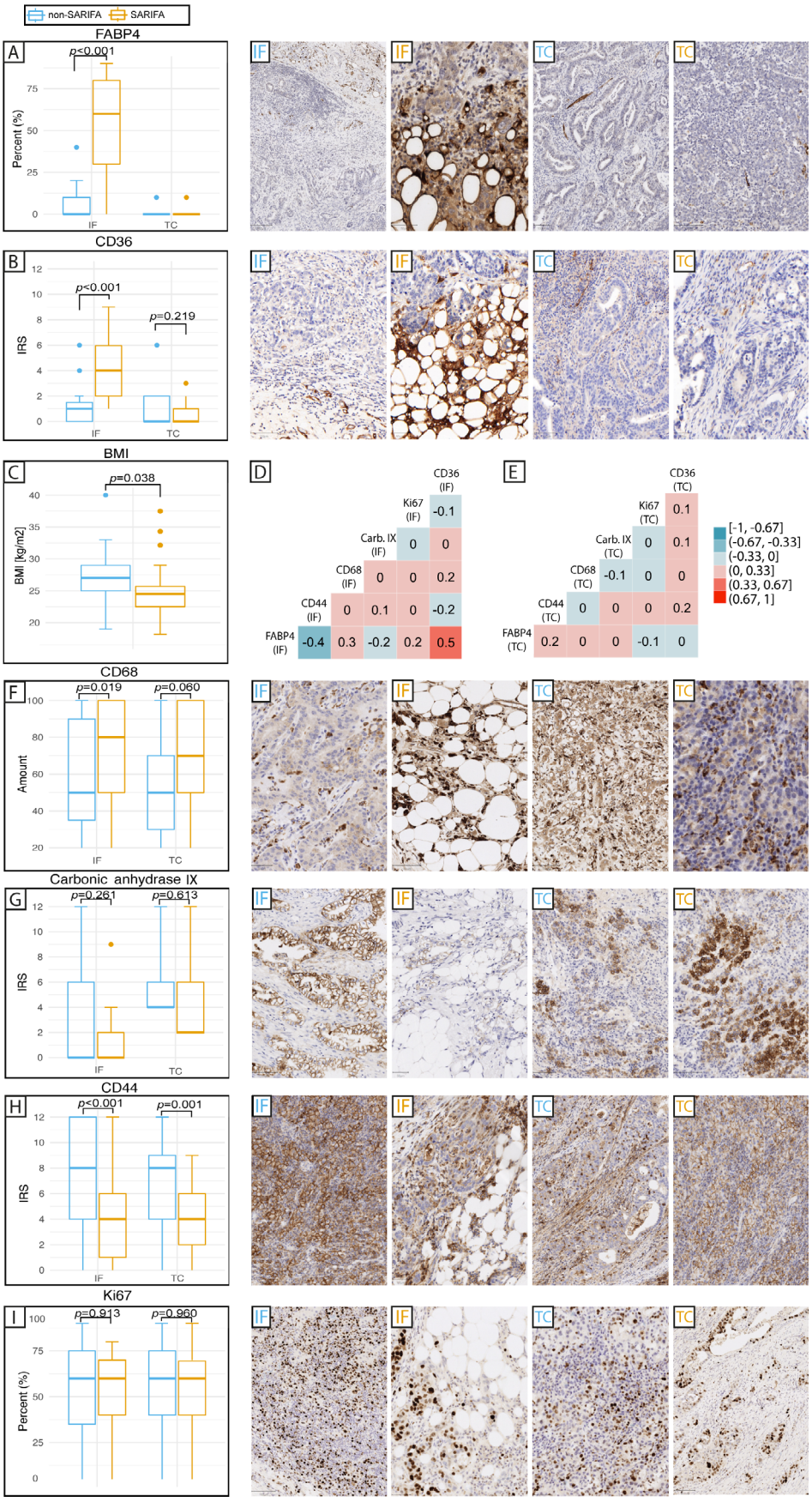

Figure 4. Immunohistochemical protein expression of differentially expressed genes in DSP analysis and of proteins associated with hypoxia and stem cell features. (A–C, F–I) Boxplots showing expression of FABP4 (A) and CD36 (B); BMI (C); (F) number of $CD68^{+}$ cells; expression of carbonic anhydrase IX (G), CD44 (H), and Ki67 (I); and examples of immunohistochemical staining. (D, E) Correlation matrix of the proteins at the IF and the TC.

correlated with the amount of $CD68^+$ cells at the IF ($\rho = 0.316$, $p = 0.019$) or in the TC ($\rho = 0.388$, $p = 0.003$) and with CD36 expression at the IF ($\rho = 0.535$, $p < 0.001$) (Figure 4D,E).

Discussion

So far, only a few prognostic and therapeutic biomarkers have been identified for gastric cancer. To date, the most important therapeutic marker in gastric carcinoma is HER2 overexpression [28]. In addition, MSI status and high PD-L1 expression are independent positive prognostic factors in gastric carcinoma [14,29,30], while aberrant E-cadherin expression is considered an unfavorable prognostic factor, and even a negative predictive factor for chemotherapy response [31]. Additionally, MET amplification and overexpression are thought to play a crucial role in gastric carcinogenesis, but this is yet to be found as a predictive factor for the response to anti-MET antibodies [14]. In this study, we present SARIFA as a new histological prognostic biomarker in gastric cancer that is easy to assess during routine diagnostic assessment. When evaluating SARIFA, there is no need for additional immunohistochemical staining or complicated evaluation schemes, such as those used for the evaluation of protein-based TCGA classification [21,22], tumor budding, the TSR [10–12], or the aforementioned prognostic biomarkers.

In addition, the criteria for SARIFA positivity are defined simply, which is reflected in the considerably low inter-observer variability with kappa values of 0.74 (Collection A) and 0.78 (Collection B) across all three observers. The presence of a single tumor cell next to inconspicuous adipocytes without the surrounding stroma is sufficient for the identification of SARIFA positivity.

SARIFA positivity was found to be a significant prognostic factor in both collections and emerged as an independent negative prognostic factor for overall survival in Collection B. As the majority of SARIFA cases are in advanced T-stage (90%), SARIFA by its nature is mainly a prognostic marker in already advanced cases. In summary, SARIFA combines a high degree of reproducibility, low additional effort, and high clinical relevance. Recently, Wulczyn *et al* [32] identified a morphologically similar phenomenon in colon carcinoma using a deep learning system.

To provide hints with regard to the underlying tumor-promoting mechanisms associated with SARIFA positivity, we conducted DSP. Among the most upregulated pathways at the IF in SARIFA-positive cases, compared with the negative cases, were those of collagen chain trimerization and fibrin clot formation. *COL15A1* was highly differentially expressed when comparing SARIFA-positive and SARIFA-negative cases. In the positive cases, its expression was also higher at the periphery than in the tumor's center. At first glance, this seems contradictory, as SARIFA-positive cases do not induce a stromal reaction and are characterized by the absence of fibrous stroma between adipocytes and tumor. *COL15A1* encodes the alpha chain of type XV collagen, which represents one component of the basement membrane (BM) and is thought to function as an adhering component between the BM and the surrounding matrix [33]. Karppinen *et al* [34] detected collagen XV in the tumor stroma during late stages of tumor progression in squamous cell carcinoma. In our DSP analysis, only the expression of tumor cells was assessed and not explicitly of the stroma. Thus, the high expression in the stroma is not an explanation for *COL15A1* expression in the tumor cells of SARIFA-positive cases. One could speculate that *COL15A1* is highly expressed because of the synthesis of a non-functional protein, resulting in inadequate collagen synthesis. But this is highly speculative and needs to be investigated in further studies. SARIFA-positive cases were associated with an increased number of CD68-positive macrophages. TAMs can polarize toward M2 macrophages that enhance angiogenesis, tumor invasion, and immune suppression [35,36]. It is therefore probable that macrophages play a role in preventing the tumor glands from being entrapped by desmoplastic fibers and induce a reduced response of the immune system in SARIFA tumors. However, the characteristics of TAMs and the polarization between M1 and M2 macrophages that are known so far are based on *in vitro* experiments and cannot be transferred without limitations *in vivo*. The exact mechanisms that lead to this phenomenon and the role of TAMs, which seem to have a great heterogeneity and comprehensive functions, remain to be elucidated [37].

Interestingly, other pathways that were significantly upregulated in SARIFA-positive cases at the IF were those of triglyceride catabolism and endogenous sterols. Certain studies in the context of obesity research have investigated the mechanisms of tumor-associated adipocytes using cell culture experiments [16,26,38]. Wen *et al* [39] report that colon cancer cells uptake fatty acids secreted by adipocytes and that adipocytes activate autophagy to support cancer cell survival by altering homeostasis and cellular metabolism in cancer cells. Among the most differentially expressed genes were fatty acid-binding proteins 2 and 4 (*FABP2* and *FABP4*). Fatty acid-binding proteins (FABPs) facilitate fatty acid transport to different cell organelles [40]. This seems to be an interesting starting point for further investigations to explain the underlying concepts of SARIFA and its association with adverse prognosis and characteristics.

To confirm the differential expression of FABP4 at the protein level, we used immunohistochemistry. We found that FABP4 was expressed almost exclusively in the tumor cells of SARIFA areas, whereas no expression was found in the TC or at the IF of SARIFA-positive and SARIFA-negative cases. Our finding regarding FABP4 expression in SARIFA areas supports the hypothesis that tumor cells gain energy through tumor fatty acid oxidation [41]. In addition, higher expression of CD36, which enables tumor cells to take up free fatty acids [26,27], was observed in the SARIFA areas. It was also observed that CD36-positive tumor cells represent a metastasis-

initiating cell population [42,43]. Thus, fatty acid oxidation provides an efficient energy source for the tumor [44]. The inhibition of this pathway could be an attractive therapeutic option. In this respect, the transport of acyl-CoAs into mitochondria by carnitine palmitoyl transferase 1 (CPT1) represents a potential target [45].

The interaction between adipocytes and tumor cells has been studied mainly in obesity research to further address the questions of why obese persons have an increased incidence of cancer with a poorer prognosis [16,38]. However, we did not observe an association between SARIFA positivity and higher BMI; on the contrary, SARIFA was even associated with lower BMI in patients (Figure 4C). Thus, obesity does not appear to be the trigger for tumor progression here. Interestingly, the tumor cells also did not appear to be affected by hypoxia, as indicated by the low expression of the hypoxia marker carbonic anhydrase IX. Further, stem cell features also do not seem to play a role in tumor progression, and there even seems to be a lower expression of the stem cell marker CD44 in SARIFA cases [46–49]. Rather, the tumor cells appear to be able to proliferate unimpeded and invade the tissue. In doing so, they benefit from their contact with adipocytes. It is possible that tumor-associated macrophages induce a reduced host tissue response. Thus, the term 'stroma areactive' describes the observed biological process quite well. The indications of SARIFA being the morphological correlate of a certain tumor biology implicate their possible role as a predictive marker for a therapy targeting TAMs or overcoming the therapy resistance created by tumor-associated fat [16,35]. In this regard, our study has certain limitations, which are mainly related to its retrospective nature. Our study has to be considered an exploratory analysis, and the results have to be validated using independent prospective cohorts.

This study presents SARIFA (Stroma Areactive Invasion Front Areas) as an extremely promising histomorphology-based prognostic factor that is related to tumor-promoting adipocytes in gastric cancer. Further studies will verify whether the results of this retrospective, single-center study can be confirmed and whether SARIFA can serve as a universal prognostic indicator for solid cancers.

Acknowledgements

We are grateful to Jenny Müller, Andrea Seuser, and Christian Beul for their excellent technical assistance. The study received no external funding. The DSP procedure was funded by the institute's internal resources; it was not directly funded by NanoString Technologies, Inc.

Author contributions statement

BM, BG and BMa contributed to the study's conception and design. MG, DV, AV, DK, SD, AP, GS and BG contributed to the data acquisition process. CD, SS, BM and BG contributed to the analysis and interpretation of data. All authors revised the article critically, contributed to it with reflective improvements, and approved the final version.

Data availability statement

The datasets generated during DSP analysis are available at https://doi.org/10.6084/m9.figshare.16615951.

References

1. Bray F, Ferlay J, Soerjomataram I, *et al*. Global cancer statistics 2018: GLOBOCAN estimates of incidence and mortality worldwide for 36 cancers in 185 countries. *CA Cancer J Clin* 2018; **68:** 394–424.
2. O'Sullivan B, Brierley J, Byrd D, *et al*. The TNM classification of malignant tumours – towards common understanding and reasonable expectations. *Lancet Oncol* 2017; **18:** 849–851.
3. In H, Solsky I, Palis B, *et al*. Validation of the 8th Edition of the AJCC TNM Staging System for Gastric Cancer using the National Cancer Database. *Ann Surg Oncol* 2017; **24:** 3683–3691.
4. Shiraishi N, Sato K, Yasuda K, *et al*. Multivariate prognostic study on large gastric cancer. *J Surg Oncol* 2007; **96:** 14–18.
5. Chen YC, Fang WL, Wang RF, *et al*. Clinicopathological variation of Lauren classification in gastric cancer. *Pathol Oncol Res* 2016; **22:** 197–202.
6. Berlth F, Bollschweiler E, Drebber U, *et al*. Pathohistological classification systems in gastric cancer: diagnostic relevance and prognostic value. *World J Gastroenterol* 2014; **20:** 5679–5684.
7. Liu K, Zhang W, Chen X, *et al*. Comparison on clinicopathological features and prognosis between esophagogastric junctional adenocarcinoma (Siewert II/III types) and distal gastric adenocarcinoma: retrospective cohort study, a single institution, high volume experience in China. *Medicine (Baltimore)* 2015; **94:** e1386.
8. Cunningham D, Allum WH, Stenning SP, *et al*. Perioperative chemotherapy versus surgery alone for resectable gastroesophageal cancer. *N Engl J Med* 2006; **355:** 11–20.
9. Allemani C, Matsuda T, Di Carlo V, *et al*. Global surveillance of trends in cancer survival 2000-14 (CONCORD-3): analysis of individual records for 37 513 025 patients diagnosed with one of 18 cancers from 322 population-based registries in 71 countries. *Lancet* 2018; **391:** 1023–1075.
10. Guo YX, Zhang ZZ, Zhao G, *et al*. Prognostic and pathological impact of tumor budding in gastric cancer: a systematic review and meta-analysis. *World J Gastrointest Oncol* 2019; **11:** 898–908.
11. Kemi N, Eskuri M, Herva A, *et al*. Tumour–stroma ratio and prognosis in gastric adenocarcinoma. *Br J Cancer* 2018; **119:** 435–439.
12. Lugli A, Zlobec I, Berger MD, *et al*. Tumour budding in solid cancers. *Nat Rev Clin Oncol* 2021; **18:** 101–115.
13. The Cancer Genome Atlas Research Network. Comprehensive molecular characterization of gastric adenocarcinoma. *Nature* 2014; **513:** 202–209.
14. Baniak N, Senger JL, Ahmed S, *et al*. Gastric biomarkers: a global review. *World J Surg Oncol* 2016; **14:** 212.
15. Martin B, Grosser B, Kempkens L, *et al*. Stroma AReactive Invasion Front Areas (SARIFA)—a new easily to determine biomarker in colon cancer-results of a retrospective study. *Cancers (Basel)* 2021; **13:** 4880.
16. Lengyel E, Makowski L, DiGiovanni J, *et al*. Cancer as a matter of fat: the crosstalk between adipose tissue and tumors. *Trends Cancer* 2018; **4:** 374–384.

17. Siewert JR, Stein HJ. Classification of adenocarcinoma of the oesophagogastric junction. *Br J Surg* 1998; **85:** 1457–1459.
18. Becker K, Mueller JD, Schulmacher C, *et al*. Histomorphology and grading of regression in gastric carcinoma treated with neoadjuvant chemotherapy. *Cancer* 2003; **98:** 1521–1530.
19. Songun I, Putter H, Kranenbarg EM, *et al*. Surgical treatment of gastric cancer: 15-year follow-up results of the randomised nationwide Dutch D1D2 trial. *Lancet Oncol* 2010; **11:** 439–449.
20. Shuster JJ. Median follow-up in clinical trials. *J Clin Oncol* 1991; **9:** 191–192.
21. Ahn S, Lee SJ, Kim Y, *et al*. High-throughput protein and mRNA expression-based classification of gastric cancers can identify clinically distinct subtypes, concordant with recent molecular classifications. *Am J Surg Pathol* 2017; **41:** 106–115.
22. Setia N, Agoston AT, Han HS, *et al*. A protein and mRNA expression-based classification of gastric cancer. *Mod Pathol* 2016; **29:** 772–784.
23. Jerby-Arnon L, Neftel C, Shore ME, *et al*. Opposing immune and genetic mechanisms shape oncogenic programs in synovial sarcoma. *Nat Med* 2021; **27:** 289–300.
24. Remmele W, Stegner HE. [Recommendation for uniform definition of an immunoreactive score (IRS) for immunohistochemical estrogen receptor detection (ER-ICA) in breast cancer tissue]. *Pathologe* 1987; **8:** 138–140 [article in German].
25. Landis JR, Koch GG. The measurement of observer agreement for categorical data. *Biometrics* 1977; **33:** 159–174.
26. Cao Y. Adipocyte and lipid metabolism in cancer drug resistance. *J Clin Invest* 2019; **129:** 3006–3017.
27. Jaqaman K, Kuwata H, Touret N, *et al*. Cytoskeletal control of CD36 diffusion promotes its receptor and signaling function. *Cell* 2011; **146:** 593–606.
28. Zhou F, Li N, Jiang W, *et al*. Prognosis significance of HER-2/neu overexpression/amplification in Chinese patients with curatively resected gastric cancer after the ToGA clinical trial. *World J Surg Oncol* 2012; **10:** 274.
29. Böger C, Behrens HM, Mathiak M, *et al*. PD-L1 is an independent prognostic predictor in gastric cancer of Western patients. *Oncotarget* 2016; **7:** 24269–24283.
30. Muro K, Chung HC, Shankaran V, *et al*. Pembrolizumab for patients with PD-L1-positive advanced gastric cancer (KEYNOTE-012): a multicentre, open-label, phase 1b trial. *Lancet Oncol* 2016; **17:** 717–726.
31. Ferreira P, Oliveira MJ, Beraldi E, *et al*. Loss of functional E-cadherin renders cells more resistant to the apoptotic agent taxol *in vitro*. *Exp Cell Res* 2005; **310:** 99–104.
32. Wulczyn E, Steiner DF, Moran M, *et al*. Interpretable survival prediction for colorectal cancer using deep learning. *NPJ Digit Med* 2021; **4:** 71.
33. Bretaud S, Guillon E, Karppinen SM, *et al*. Collagen XV, a multifaceted multiplexin present across tissues and species. *Matrix Biol Plus* 2020; **6–7:** 100023.
34. Karppinen SM, Honkanen HK, Heljasvaara R, *et al*. Collagens XV and XVIII show different expression and localisation in cutaneous squamous cell carcinoma: type XV appears in tumor stroma, while XVIII becomes upregulated in tumor cells and lost from microvessels. *Exp Dermatol* 2016; **25:** 348–354.
35. Zhou J, Tang Z, Gao S, *et al*. Tumor-associated macrophages: recent insights and therapies. *Front Oncol* 2020; **10:** 188.
36. Di Caro G, Cortese N, Castino GF, *et al*. Dual prognostic significance of tumour-associated macrophages in human pancreatic adenocarcinoma treated or untreated with chemotherapy. *Gut* 2016; **65:** 1710–1720.
37. Wu K, Lin K, Li X, *et al*. Redefining tumor-associated macrophage subpopulations and functions in the tumor microenvironment. *Front Immunol* 2020; **11:** 1731.
38. Quail DF, Dannenberg AJ. The obese adipose tissue microenvironment in cancer development and progression. *Nat Rev Endocrinol* 2019; **15:** 139–154.
39. Wen YA, Xing X, Harris JW, *et al*. Adipocytes activate mitochondrial fatty acid oxidation and autophagy to promote tumor growth in colon cancer. *Cell Death Dis* 2017; **8:** e2593.
40. Thumser AE, Moore JB, Plant NJ. Fatty acid binding proteins: tissue-specific functions in health and disease. *Curr Opin Clin Nutr Metab Care* 2014; **17:** 124–129.
41. Huang J, Duran A, Reina-Campos M, *et al*. Adipocyte p62/SQSTM1 suppresses tumorigenesis through opposite regulations of metabolism in adipose tissue and tumor. *Cancer Cell* 2018; **33:** 770–784.e6.
42. Pascual G, Avgustinova A, Mejetta S, *et al*. Targeting metastasis-initiating cells through the fatty acid receptor CD36. *Nature* 2017; **541:** 41–45.
43. Ladanyi A, Mukherjee A, Kenny HA, *et al*. Adipocyte-induced CD36 expression drives ovarian cancer progression and metastasis. *Oncogene* 2018; **37:** 2285–2301.
44. Iwamoto H, Abe M, Yang Y, *et al*. Cancer lipid metabolism confers antiangiogenic drug resistance. *Cell Metab* 2018; **28:** 104–117.e5.
45. Zaugg K, Yao Y, Reilly PT, *et al*. Carnitine palmitoyltransferase 1C promotes cell survival and tumor growth under conditions of metabolic stress. *Genes Dev* 2011; **25:** 1041–1051.
46. Bayik D, Lathia JD. Cancer stem cell–immune cell crosstalk in tumour progression. *Nat Rev Cancer* 2021; **21:** 526–536.
47. Zöller M. CD44: can a cancer-initiating cell profit from an abundantly expressed molecule? *Nat Rev Cancer* 2011; **11:** 254–267.
48. Akhavan-Niaki H, Samadani AA. Molecular insight in gastric cancer induction: an overview of cancer stemness genes. *Cell Biochem Biophys* 2014; **68:** 463–473.
49. Brabletz T, Kalluri R, Nieto MA, *et al*. EMT in cancer. *Nat Rev Cancer* 2018; **18:** 128–134.
50. Bronsert P, Kohler I, Timme S, *et al*. Prognostic significance of Zinc finger E-box binding homeobox 1 (ZEB1) expression in cancer cells and cancer-associated fibroblasts in pancreatic head cancer. *Surgery* 2014; **156:** 97–108.
51. Köbel M, Piskorz AM, Lee S, *et al*. Optimized p53 immunohistochemistry is an accurate predictor of *TP53* mutation in ovarian carcinoma. *J Pathol Clin Res* 2016; **2:** 247–258.
52. Grosser B, Kohlruss M, Slotta-Huspenina J, *et al*. Impact of tumor localization and molecular subtypes on the prognostic and predictive significance of p53 expression in gastric cancer. *Cancers (Basel)* 2020; **12:** 1689.

References 50–52 are cited only in the supplementary material.

SUPPLEMENTARY MATERIAL ONLINE

Supplementary materials and methods

Table S1. Antibodies and dilutions used

Table S2. Cox regression analyses

Table S3. Subgroup analyses: Cox regression analyses